

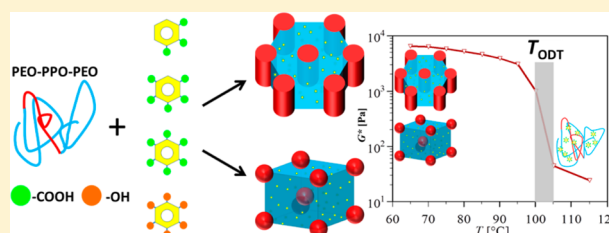
# Rheological Study of Order-to-Disorder Transitions and Phase Behavior of Block Copolymer–Surfactant Complexes Containing Hydrogen-Bonded Small Molecule Additives

Rohit Kothari,<sup>†</sup> H. Henning Winter,<sup>‡</sup> and James J. Watkins<sup>\*†</sup>

<sup>†</sup>Department of Polymer Science & Engineering and <sup>‡</sup>Department of Chemical Engineering, University of Massachusetts, Amherst, Massachusetts 01003, United States

## Supporting Information

**ABSTRACT:** Dynamic mechanical measurements were used to investigate the effect of small molecule additives on the order-to-disorder transitions (ODTs) of Pluronic, poly(ethylene oxide) (PEO)–poly(propylene oxide) (PPO)–PEO triblock copolymer surfactant melts. The small molecule additives contain multiple functional groups (carboxyl or hydroxyl), which selectively interact with the PEO component of Pluronic via hydrogen bonding, thereby effectively increasing  $\chi$  of the system and leading to microphase separation in otherwise disordered melts. The ODTs of these Pluronic/small-molecule-additive complexes can be detected by rheology since, upon increasing temperature, crossing the order-to-disorder transition temperature ( $T_{\text{ODT}}$ ) results in a sharp decrease in the low frequency storage and loss moduli ( $G'$  and  $G''$ , respectively). The crystallization of the PEO component is suppressed with increasing additive loading due to strong hydrogen bond interactions. The  $T_{\text{ODT}}$  is strongly composition dependent and increases up to 145 °C for 20 wt % loading of a particular additive.  $T_{\text{ODT}}$  is also found to vary widely but systematically with the number, position and hydrogen-bond-donating ability of the functional groups of the additive. Upon increasing temperature for high additive loadings, macrophase separation and crystallization of the additives can occur before the ODT is detected.



## INTRODUCTION

The phase behavior of block copolymers (BCPs) with two chemically distinct molecular segments is governed by the relative volume fraction of the blocks and the product  $\chi N$ , where  $\chi$  and  $N$  are the Flory–Huggins interaction parameter of the blocks and the degree of polymerization, respectively.<sup>1</sup> Microphase separation into ordered morphologies (lamellar, bicontinuous, cylindrical and spherical) occurs below the  $T_{\text{ODT}}$  for sufficiently large  $\chi N$ .<sup>2,3</sup> Self-assembly of BCPs into nanostructured morphologies facilitates their use as materials for the fabrication of high density data storage media,<sup>4–7</sup> high resolution etch masks,<sup>8,9</sup> nanopores,<sup>10,11</sup> nanowires,<sup>12</sup> and nanopillars,<sup>13</sup> and as templates for mesoporous inorganic materials.<sup>14–16</sup> The increasing demand for higher density microelectronic structures and the associated well-ordered morphologies with small features (3–15 nm) requires increasing  $\chi$ , to compensate for small  $N$ , in order to maintain a sufficiently large  $\chi N$ .

Hydrogen bonding is one of the key mechanisms behind the formation of various supramolecular structures from small moieties. Taking advantage of versatility, directionality, and stability of the interactions, hydrogen bonding between small molecule building blocks has enabled researchers to create supramolecular assemblies exhibiting liquid crystalline behavior.<sup>17–22</sup> Hydrogen bond assisted liquid crystalline supramolecular assemblies have also been achieved in blends containing polymers and mesogenic<sup>23–27</sup> or nonmesogenic<sup>28</sup>

small molecules. Hierarchical assemblies at two different length scales have been demonstrated by the means of selective hydrogen bonding between mesogenic or amphiphilic additive molecules and a specific block of the block copolymers.<sup>29–36</sup> Disorder-to-order<sup>33</sup> and order-to-order<sup>29–34</sup> transitions in the block copolymer can be introduced through the loading of the additive molecules. Owing to the mesogenic or amphiphilic nature, these additive molecules further self-organize within the host domain of the microphase separated block copolymers to result in composition dependent hierarchical morphologies.

Recently, it has been shown that multiple-hydrogen-bond-donating small molecules can selectively associate with a particular block and induce microphase separation in otherwise disordered BCPs.<sup>37</sup> The molecules used are nonmesogenic and nonamphiphilic, therefore no substructures are formed within the resulting microphase separated domains and the morphologies native to the block copolymers are preserved. The resulting well-ordered morphologies exhibit feature sizes of less than 15 nm, which is important for applications requiring small domains. Since the microphase separation is driven by the addition of the small molecule component, segregation strength, and consequently the order-to-disorder transition temperature ( $T_{\text{ODT}}$ ) will naturally depend upon the strength

Received: September 4, 2014

Revised: October 24, 2014

and the number of hydrogen bond interactions presented by the additive and the loadings of the small molecule additive into the BCP. Studying ODTs in these BCP/small-molecule-additive complexes is of particular interest.

Block copolymers of PEO and PPO are commercially available under the trade name Pluronic. The hydrophobic PPO block and the hydrophilic PEO block give the molecule an amphiphilic nature typical of a nonionic surfactant. Pluronic block copolymers are usually disordered at room temperature and above in the melt due to their low molecular weight and weak repulsive interaction between PEO and PPO blocks. By taking advantage of the hydrogen bonding interaction, microphase separation can be induced by blending Pluronic block copolymers with homopolymers,<sup>38</sup> small molecule additives,<sup>37</sup> and functionalized nanoparticles.<sup>39</sup> All of these additives bear hydrogen bond donating sites which selectively interact with the hydrophilic PEO blocks, increasing the effective  $\chi$  parameter and thus leading to microphase separation.

Upon gradual addition of small molecule additives, such as benzenehexacarboxylic acid or hexahydroxybenzene, into Pluronic F108, transition from disordered morphology to cylindrical morphology was observed through small-angle X-ray scattering (SAXS).<sup>37</sup> Further addition of additive induced the transition from cylindrical to spherical morphologies, followed by macrophase separation of the additive at a very high loading (>40 wt % in case of benzenehexacarboxylic acid). By comparing full width at half-maximum of the primary peaks of the SAXS profiles and domain spacing for ordered cylindrical morphologies, it was shown that additives bearing carboxyl functional groups compared to hydroxyl groups exhibit a stronger capacity to increase segregation strength and induce microphase separation.

In this study we used rheology to explore the temperature-dependent phase behavior of Pluronic F108 over a broad range of small molecule loadings. The phase behavior is essentially different from that of neat BCP due to the additional component (small molecule) which drives microphase separation via hydrogen bonding interaction. Interestingly, macrophase separation of additive was observed at high temperature. A set of small molecule additives with an identical core but systematic variance in the number of carboxyl functional groups was utilized to explore the dependence of  $T_{ODT}$  upon the number of hydrogen bonding sites presented by the additive. The change in  $T_{ODT}$  by changing the type of functional group on the additive was studied by blending additives with similar structure, but different functionality, carboxyl or hydroxyl.

Nanoparticles decorated with functional small molecules have been demonstrated to drive microphase separation in BCPs.<sup>39,40</sup> Hydrogen bonding is the key that allow high loadings of inorganic nanoparticles to self-assemble in desired domain of BCP. There is a need to determine physical properties and understand the rheological behavior of these technologically promising hybrid nanocomposites. With the insight gained from exploring the self-assembly of a BCP as a function of the number and the type of functional group on a small molecule, one can advance the development and processing of hybrid nanocomposites with inorganic fillers bearing such functional small molecules.

## EXPERIMENTAL SECTION

**Materials.** The PEO–PPO–PEO Pluronic F108 (F108) was donated by BASF. Its hydrophilic PEO side blocks comprise 80 wt % of the molecule. The hydrophobic PPO middle block has an average molecular weight of about 3 kg/mol. Dispersity of F108 as determined by gel permeation chromatography was 1.2. Poly(ethylene oxide) (PEO) homopolymer ( $M_w = 20$  kg/mol) was obtained from Sigma-Aldrich. Small molecule additives, Figure 1, benzene-1,2,3,4,5,6-

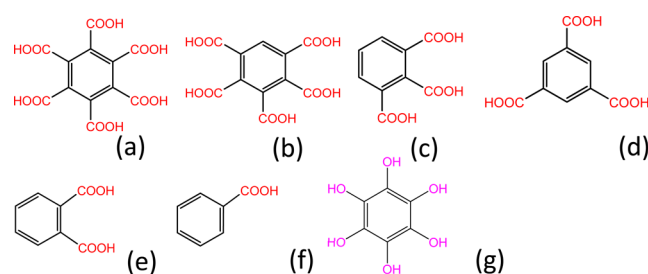


**Figure 1.** Additives used in this study: (a) benzene-1,2,3,4,5,6-hexacarboxylic acid (BHCA), (b) benzene-1,2,3,4,5-pentacarboxylic acid (BPCA), (c) benzene-1,2,3-tricarboxylic acid (123BTCA), (d) benzene-1,3,5-tricarboxylic acid (135BTCA), (e) phthalic acid, (f) benzoic acid, and (g) benzene-1,2,3,4,5,6-hexol (HHB).

hexacarboxylic acid (BHCA), benzene-1,2,3,4,5-pentacarboxylic acid (BPCA), benzene-1,2,3-tricarboxylic acid (123BTCA) hydrate, benzene-1,3,5-tricarboxylic acid (135BTCA), and benzene-1,2,3,4,5,6-hexol (HHB) were purchased from TCI America. Phthalic acid and benzoic acid were purchased from Sigma-Aldrich. Reagent grade water and *N,N*-dimethylformamide (DMF) used as solvents were obtained from Fisher Scientific. 123BTCA was heated at 100 °C under vacuum for several hours to remove water of crystallization. Otherwise, the materials and solvents were used as received.

**Sample Preparation.** Appropriate amounts of F108 and small molecule additives were blended by solution casting from a 1:1 weight ratio mixture of water and DMF. Clear solutions of 15 wt % solids were transferred to a 60 mm diameter glass Petri dish, heated to 60 °C for 48 h, and further dried in vacuum at 60 °C for 24 h to remove residual solvent. Batch sizes and preparation protocols were strictly adhered to minimize deviations that might occur due to variation in solvent evaporation rate and thermal history. Additionally, a blend containing 65 wt % PEO and 35 wt % BHCA was prepared using the same protocol.

A blend represented as  $x/y$  is composed of  $x$  wt % F108 and  $y$  wt % of small molecule additive ( $x + y = 100$ ). For the purpose of comparison of  $T_{ODT}$  between different F108/additive blends, additives are blended in amounts that maintain equivalent numbers of functional groups per gram of F108. For example, to incorporate 30 mequiv carboxyl groups per gram of F108, the amount of BHCA added will be 5 mequiv, the amount of BPCA added will be 6 mequiv and the amount of 123BTCA added will be 10 mequiv. As a consequence, the mass fraction and the volume fraction of the additive incorporated per gram of F108 increase accordingly. This volume effect will be discussed further in connection with the experimental results.

**Rheometry.** Dynamic mechanical measurements were performed on an ARES (Rheometric Scientific) strain-controlled rotational rheometer, using parallel plate fixtures of 25 mm diameter. Pellets of dried samples were heated at 60 °C and squeezed between rheometer fixtures to a gap size of 0.6 mm. Small amplitude oscillatory shear (strain amplitude  $\gamma = 0.01$ ) was applied in the linear viscoelastic regime. To locate ODT, isothermal frequency sweeps over four decades of frequency ( $0.01$  rad/s  $< \omega < 100$  rad/s) were performed at increasing temperature with steps of 5 K. Interactive IRIS (2006) software was used to analyze and plot the rheological data.

**Small Angle X-ray Scattering (SAXS).** SAXS was performed on Rigaku-Molecular Metrology SAXS equipment using Cu  $K\alpha$  radiation

having wavelength  $\lambda = 0.1542$  nm. The size of incident beam at sample position was approximately 4 mm in diameter. A two-dimensional detector recorded SAXS patterns in a  $q$  range  $0.06$ – $1.5$  nm $^{-1}$ , where the scattering vector is defined as  $q = (4\pi/\lambda)(\sin \theta)$ ,  $2\theta$  being scattering angle. The distance between sample and detector was calibrated using the silver behenate's primary diffraction peak at  $q = 1.076$  nm $^{-1}$ . Samples were placed between 2 mm thick steel washers and sealed from both sides using a thin Kapton film. Experiments were performed by heating samples under vacuum to a fixed temperature using a Linkam hot stage. Isothermal scattering data was circularly averaged and plotted as intensity vs  $q$  where intensity was in arbitrary units. Data are shifted vertically by constant factors to avoid overlap.

**Differential Scanning Calorimetry (DSC).** DSC was carried out to obtain melting enthalpies of the PEO crystallites present in blends. Samples weighing around 10 mg were filled into hermetic aluminum pans and sealed. Experiments were performed on TA Instruments Q200 DSC equipped with refrigerated nitrogen cooling system and nitrogen gas purge flow rate of 50 mL/min. Temperature and heat flow were calibrated using indium as a standard. All measurements were conducted in the temperature range of  $-50$  to  $80$  °C with heating and cooling rate of 10 and 1 K/min, respectively. The reported DSC thermograms were measured during second heating cycles.

## RESULTS AND DISCUSSION

All of the small molecule additives (Figure 1) are crystalline at room temperature and show no melting or degradation in the experimental temperature window for this study. We start by elaborating the phase behavior of F108/BHCA in detail to establish generality in these hydrogen-bonded F108/small-molecule-additive complexes. Out of all additives used here, BHCA induced the strongest segregation in F108. The influence of all other additives on segregation strength will be measured against BHCA by comparing  $T_{\text{ODT}}$  of their respective blends with F108 to  $T_{\text{ODT}}$  of F108/BHCA.

**ODT and Phase Behavior in F108/BHCA Complexes.** Figure S1 in the Supporting Information provides SAXS measurements and isothermal frequency sweep on neat F108 at  $65$  °C, at a temperature slightly above the melting point of the PEO segments. In SAXS, F108 shows a broad hump consistent with a disordered morphology. In rheological measurement the material shows the characteristic of a melt with  $G'$  and  $G''$  being frequency dependent and  $G'$  being less than  $G''$ .

The enthalpy of melting of PEO (integrated area under the melting endotherms) decreases upon the addition of BHCA to F108, as shown in Figure 2 (inset). This indicates the existence of favorable hydrogen bonding interactions, which result in molecular level mixing of the additive with PEO chains, thereby suppressing PEO crystallization. The enthalpy of fusion is normalized to PEO content in the blends; for neat F108 it was found to be 165 J/g of PEO. The percentage crystallinity with respect to neat F108 is calculated and plotted in Figure 2. For example, upon adding 20 wt % of additive we see around 80% reduction in the crystallizable PEO phase. Owing to the high compatibility between BHCA and PEO, loading of the additive can be further increased to 40 wt % without macrophase separation of the additive in the as prepared sample.

The strong interactions between multiple-hydrogen-bond-donating BHCA molecules and multiple-hydrogen-bond-accepting PEO chains persists well above the melting temperature of PEO. The addition of BHCA to the PEO chains increases the repulsion of PEO with the PPO segments and leads to microphase separation by creation of BHCA-PEO microdomains and PPO microdomains. In absence of BHCA, weak repulsion of PEO with PPO upon melting would cause the material to be disordered ( $\chi_{\text{BHCA/PEO-PPO}}^N > \chi_{\text{PEO-PPO}}^N$ ).

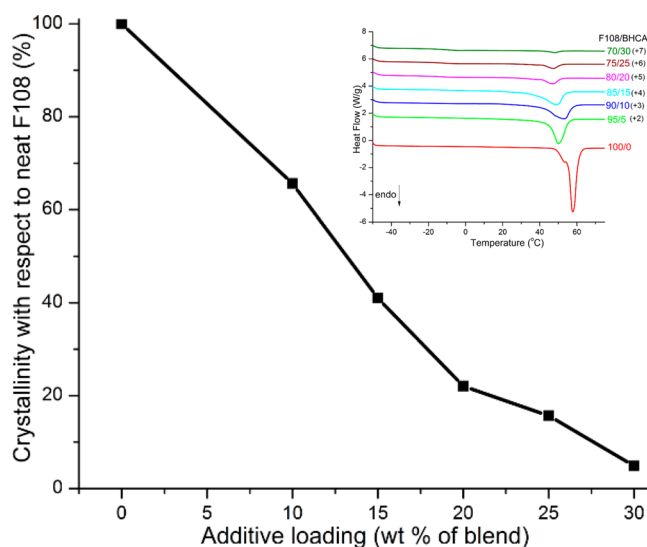


**Figure 2.** Percent crystallinity of poly(ethylene oxide) (PEO) in the blends containing Pluronic F108 (F108) and benzene-1,2,3,4,5,6-hexacarboxylic acid (BHCA) plotted against the loadings of BHCA in the blends. The percent crystallinity of PEO in the blends is presented with respect to percent crystallinity of PEO in neat F108, which is arbitrarily set to 100%. The inset shows DSC thermograms of the blends. Thermograms except that of neat F108 were shifted vertically by constant factors (indicated in brackets) to avoid overlap.

Isothermal frequency sweeps conducted on 90/10 F108/BHCA blends are shown in Figure 3a. For temperatures below  $100$  °C the material is microphase separated, exhibiting solid-like behavior with  $G'$  and  $G''$  weakly depending upon frequency.<sup>41–46</sup> Upon heating to  $100$  °C,  $G'$  decreases slightly due to lattice softening. Between  $100$  and  $105$  °C,  $G'$  and  $G''$  decrease by several orders of magnitude, as expected for ODT. At  $105$  °C and above,  $G'$  and  $G''$  strongly depend on frequency with  $G' < G''$  depicting liquid-like behavior.<sup>41–46</sup> The rheometer torque at low frequency in the disordered region is too low to yield a good signal/noise ratio, leading to scattered data. The melting of the structure is most clearly seen when plotting the complex modulus ( $G^*$ ) against temperature at different frequencies, as shown in Figure 3b. The sharp decrease of  $G^*$  for the low frequencies between  $100$  and  $105$  °C represents ODT. The Winter plot,<sup>47</sup> Figure 3c shows the transition even more dramatically. The solid like ordered morphology results in a nearly vertical  $\eta^*$  when plotted over  $G^*$ , while the disappearance of order results in a nearly horizontal  $\eta^*$  on the Winter plot. The morphology transition was confirmed using SAXS before and after ODT ( $100$ – $105$  °C). For temperatures up to  $100$  °C, a sharp primary peak and higher order peaks indicate cylindrical morphology, with a principal domain spacing,  $d = 2\pi/q^* \approx 14$  nm as shown in Figure 4. A broad hump at  $110$  °C confirms disordered morphology as seen in rheology.

It is important to note that, at low temperatures, the blend acts as physical gel (solid-like behavior) due to microphase separation and not due to formation of a network structure by multiple-hydrogen-bonding interaction between PEO chains and BHCA molecules. This is supported by dynamic mechanical measurements on a blend containing 35 wt % BHCA and 65 wt % PEO homopolymer ( $M_w = 20$  kg/mol), where hydrogen bond network formation occurs but microphase separation is not a possibility. This loading of BHCA in

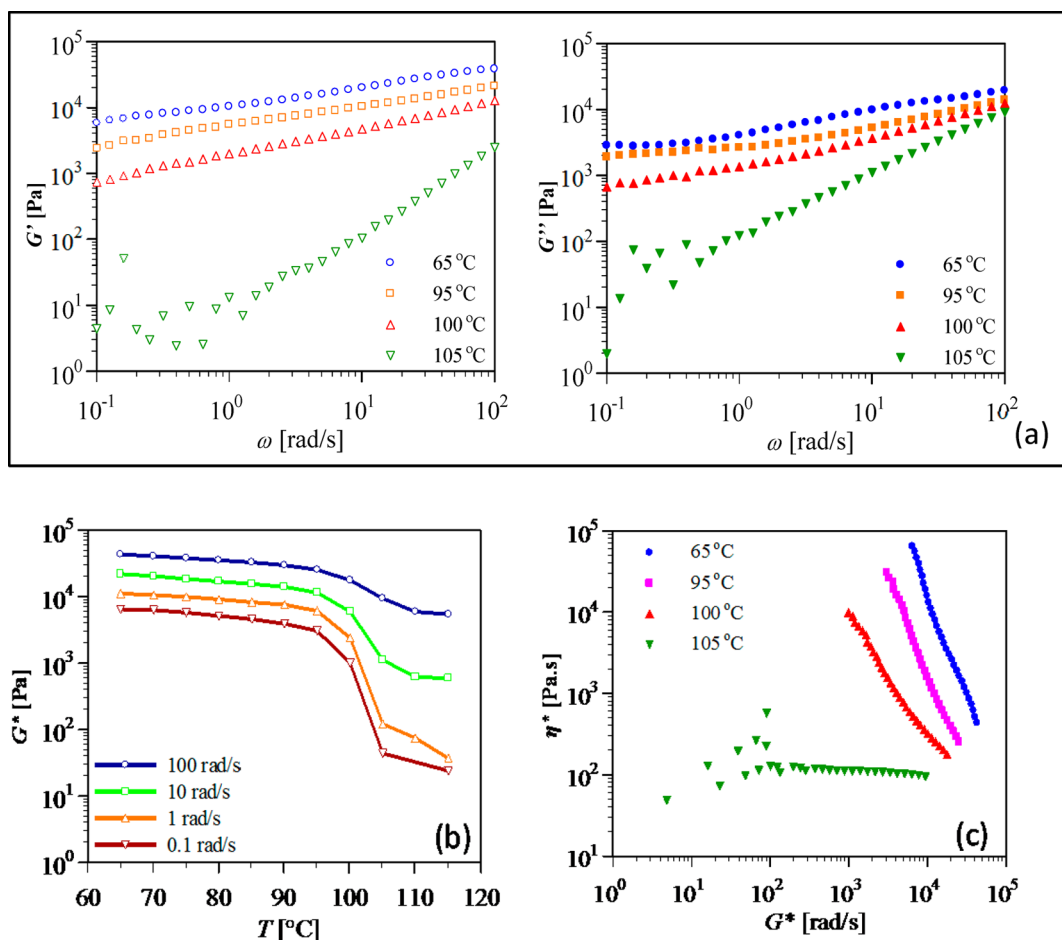


**Figure 3.** Rheology plots for determining order-to-disorder transition temperature ( $T_{\text{ODT}}$ ) for blends containing 90 wt % Pluronic F108 (F108) and 10 wt % benzene-1,2,3,4,5,6-hexacarboxylic acid (BHCA) (a) Isothermal frequency sweeps of storage modulus ( $G'$ ), on left, and loss modulus ( $G''$ ), on right at various temperatures.  $T_{\text{ODT}}$  occurs between 100 and 105 °C. Low frequency moduli at 105 °C are too small to allow good signal/noise ratios as indicated by scattered data points. (b) Complex modulus ( $G^*$ ) vs temperature at different angular frequencies for the same blend. The sharp drop in  $G^*$  between 100 and 105 °C, most pronounced at lower frequencies, represents ODT. (c) Complex viscosity ( $\eta^*$ ) vs  $G^*$  at different temperatures. The ODT is characterized by sharp change in the dependence of  $\eta^*$  on  $G^*$  between 100 and 105 °C.  $\eta^*$  is strongly dependent on  $G^*$  at temperatures of 100 °C and lower, but is weakly dependent on  $G^*$  at 105 °C and higher temperature.

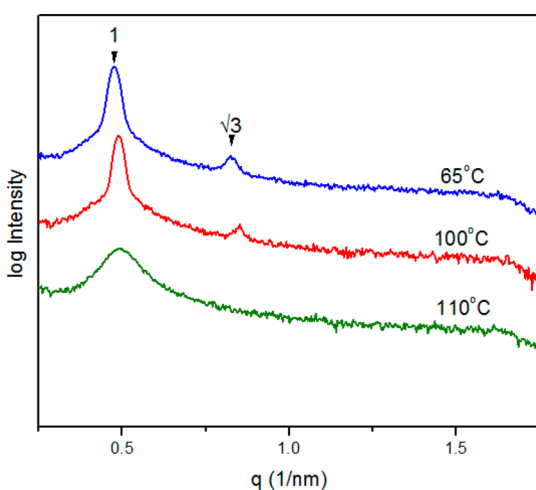


**Figure 4.** Small angle X-ray scattering (SAXS) profiles at various temperatures for blend containing 90 wt % Pluronic F108 (F108) and 10 wt % benzene-1,2,3,4,5,6-hexacarboxylic acid (BHCA). Intensity is in arbitrary units and profiles are shifted vertically to avoid overlap. Microphase separation results in cylindrical morphologies at 100 °C and below with  $q/q^* \sqrt{3}:1$ . The blend disorders at 110 °C and above.

PEO is higher compared to the loading in PEO phase of F108 in any of the blends used in this study. Unlike gels, this blend shows strong frequency-dependent viscoelastic behavior with  $G' < G''$  in the low frequency regime (Supporting Information, Figure S2) at 65 °C, a temperature slightly above the melting of PEO.

$T_{\text{ODT}}$  was found to rapidly increase up to 145 °C for up to 20 wt % loading, Figure 5. A blend with 5 wt % additive is disordered above 60 °C. Below this temperature,  $T_{\text{ODT}}$  could not be determined due to the crystallization of the PEO blocks. With increased BHCA loading, number of hydrogen bonding interactions between BHCA molecules and PEO chains increases which in turn leads to an increased  $\chi N_{\text{BHCA/PEO-PPO}}$  and higher  $T_{\text{ODT}}$ . There is no appreciable increase in  $T_{\text{ODT}}$  on further increasing the additive loading. This may be a consequence of two factors, the concentration of additives is high enough such that interactions occur with all available hydrogen bond accepting sites on the polymer and a weakening of the strength of the hydrogen bonds between carboxyl group proton and ether oxygen in PEO as temperature increases. It is likely that these weakening interactions trigger self-association of the additive molecules leading to the formation of crystals at elevated temperatures.

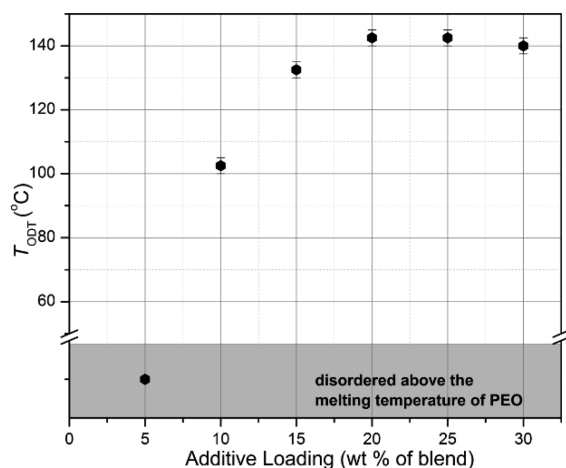


**Figure 5.** Order-to-disorder transition temperature ( $T_{ODT}$ ) dependence on benzene-1,2,3,4,5,6-hexacarboxylic acid (BHCA) loading in blends containing Pluronic F108 (F108) and BHCA.

There are certain conditions under which the additive crystallizes instead of forming complexes with F108. For highly loaded systems the additive self-associates and forms crystals at sufficiently high temperature. For a blend containing 25 wt % BHCA beyond its  $T_{ODT}$  (140–145 °C), the modulus increased as shown in Figure 6a. A small change in  $G^*$  over a wide range of frequency at 170 °C shows that material is again acting as a gel after having passed through a solid to liquid transition at  $T_{ODT}$ . This increase in modulus and physical gelation is due to the formation of sufficiently large crystallites of additive creating reinforcement. The crystals act as physical cross-linking sites that hinder polymer chain segmental motion and lock the disordered morphology. Crystallization induced turbidity in the blends and was confirmed using cross-polarized optical microscopy (Supporting Information, Figure S3). Note that the temperatures at which macrophase separation occurs remain well below the melting point (higher than 280 °C) of the additive crystals. Moreover, the additive crystals tend to remain undissolved upon cooling back to room temperature.

Blends with over 30 wt % BHCA are no longer homogeneous before  $T_{ODT}$  is reached. For example, 68/32

F108/BHCA blends did not show any signature of an ODT. In Figure 6b, there is negligible change in  $G^*$  upon increasing temperature from 70 to 140 °C. Heating from 140 to 145 °C causes  $G^*$  to decrease slightly but  $G^*$  increases again upon further heating beyond 150 °C and almost regains its initial values upon heating to 170 °C. Upon further increasing BHCA loading to 40 wt %, the blends assume spherical morphologies (Supporting Information, Figure S4), as detected by SAXS. Again, ODTs cannot be detected due to crystallization of the additives at higher temperature. Complexes with BHCA loadings of 50 wt % and more cannot be achieved as BHCA crystallizes and macrophase separate during solvent removal. Similar macrophase separation of crystals at high temperature has been observed for pentadecylphenol, which forms hydrogen bonds with methanesulfonic acid functionalized poly(4-vinylpyridine).<sup>29</sup>

**Comparison of ODT in Different F108/Small-Molecule-Additive Complexes.** The rigid Pluronic BCP/small-molecule-additive complexes serve as model systems to study the effect of number and strength of hydrogen bonding interactions on  $T_{ODT}$  as determined by rheology, as described earlier. The additives shown in Figure 1 were selected for their different number of hydrogen bonding functional groups (carboxyl) while maintaining the same noninteracting core (benzene ring). As  $T_{ODT}$  is directly related to the segregation strength, rheology enables us to compare the effectiveness of additives for inducing microphase separation in these blends. For comparison purpose, additives are blended into F108 in amounts that maintain constant milliequivalents of functional groups so as to have nearly the same number of enthalpic interaction sites per gram of F108. The corresponding milliequivalents of functional group incorporated per gram of F108 and the resulting morphology type as determined by SAXS at 60 °C are indicated next to each data point in Figure 7. We observed a significant reduction in  $T_{ODT}$  when reducing the number of hydrogen bonding sites available on the additives, while keeping the total number of hydrogen bonding sites the same in all blends. A change of number of functional groups on the additive from 6 to 5 and from 6 to 3 respectively lowers the  $T_{ODT}$  by  $\sim 20$  and  $\sim 80$  °C. The influence of entropic penalties resulting from the chain stretching of PEO to accommodate the

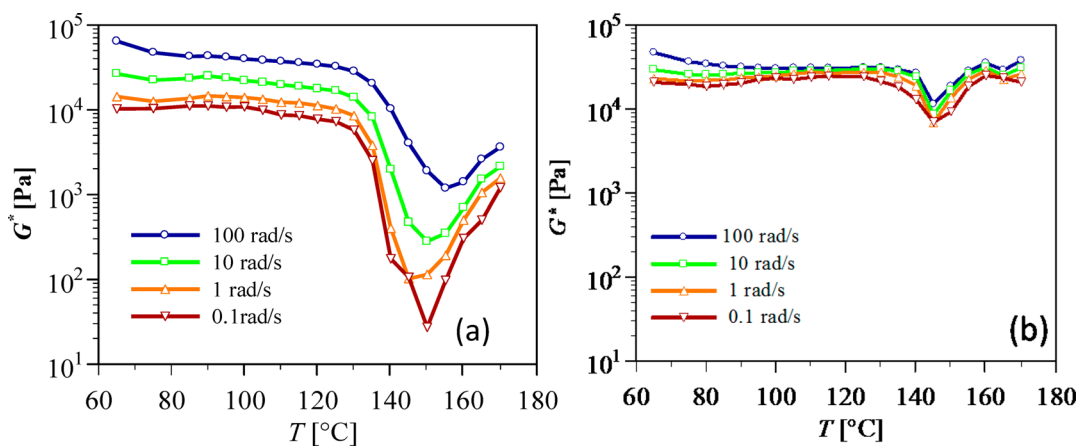


**Figure 6.** Complex modulus ( $G^*$ ) vs temperature at different angular frequencies for a blend containing (a) 75 wt % Pluronic F108 (F108) and 25 wt % benzene-1,2,3,4,5,6-hexacarboxylic acid (BHCA). The blend goes through an order-to-disorder transition (ODT) at around 145 °C with the low frequency  $G^*$  dropping several orders of magnitude.  $G^*$  starts increasing again beyond ODT due to BHCA crystallization causing physical gelation. (b) Blends containing 68 wt % F108 and 32 wt % BHCA shows a slight drop in  $G^*$  at around 145 °C resembling an onset of ODT. A complete signature of ODT is not seen when further heating as  $G^*$  increases quickly due to BHCA crystallization.

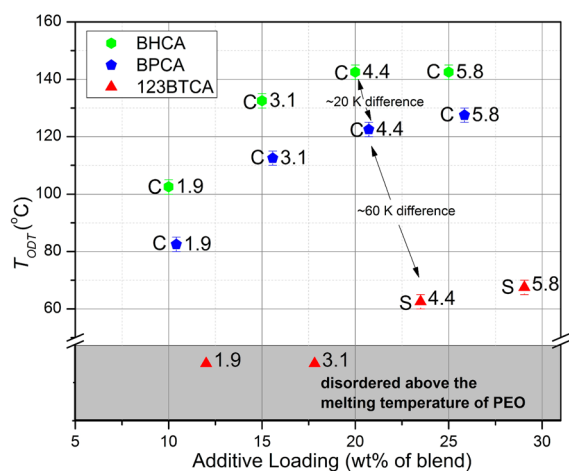


**Figure 7.** Order-to-disorder transition temperature ( $T_{ODT}$ ) dependence on additive loading for blends containing Pluronic F108 (F108) and three different additives from Figure 1, BHCA, BPCA and 123BTCA. Character next to each data point represents morphology of the blend at 60 °C, “C”-cylindrical morphology and “S”-spherical morphology. The digit next to each data point represents milliequivalents of carboxyl functional group incorporated per gram of F108 in the blend.

additive molecules also favor decreases in segregation strength. To keep the total number of hydrogen bonding sites constant, 123BTCA is added in highest volume fraction followed by BPCA, and then BHCA. The simulated Connolly solvent excluded volumes of these molecules can be related to volume that they will occupy in the PEO phase. These are 164, 152, and 135 Å<sup>3</sup> for BHCA, BPCA, and BTCA respectively.<sup>48</sup> For example, for 30 functional groups loaded into F108, the number of molecules of added would be 5 for BHCA, 6 for BPCA, and 10 for 123BTCA. This provides that for a given number of enthalpic interactions the volume of BPCA and 123BTCA would be 1.1 times and 1.6 times that of the volume of BHCA, respectively. Although differences in BHCA and BPCA are small, 123BTCA differs significantly and therefore F108/123BTCA blends assume spherical morphologies at low loading percentages, at which F108/BHCA and F108/BPCA blends are in the cylindrical morphology region.

It has been reported that the acidic strength of a functional group is directly proportional to hydrogen bonding strength.<sup>49</sup> Therefore, in these blends, it is a key factor affecting segregation strength.  $pK_a$  values indicate 123BTCA ( $pK_a^1$  2.88) is a weaker acid than BHCA ( $pK_a^1$  1.80)<sup>50,51</sup> and therefore forms a weaker hydrogen bond. 123BTCA crystallization has been observed in blends at temperature as low as 80 °C. Though BHCA, BPCA, and 123BTCA forms homogeneous blends for concentration explored up to 30 wt %, phthalic acid, and benzoic acid precipitates out even at 5 wt % loadings. More interestingly benzene 135BTCA also precipitates out at 5 wt % loadings in spite of having same number of functional groups as 123BTCA. There is a competition between the interaction of additive molecules with PEO and with themselves. Additives with weak and insufficient numbers of hydrogen bonding sites upon blending with F108 do not have enough overall hydrogen bonding interaction with the polymer to overcome its crystallization. Moreover, the additive molecules have different crystallization energies owing to difference in molecular structure and packing. Therefore, 135BTCA, being planar, precipitates out whereas 123BTCA

(nonplanar) does not. Benzene-1,2,3,4,-tetracarboxylic acid was not used in this study due to its sparse commercial availability and complex synthesis. Benzene-1,2,4,5,-tetracarboxylic has poor solubility in PEO, similar to 135BTCA and phthalic acid.

Next, we compare the capacity of carboxyl and hydroxyl to induce microphase separation, as measured in terms of  $T_{ODT}$ . BHCA and HHB, both contain a benzene ring and six carboxyl and hydroxyl functional groups respectively and are suitable molecules for comparing the effect of these functional group on  $T_{ODT}$ . We blend BHCA and HHB into F108 in an amount to provide the same number of these hydrogen bonding functional groups per gram of F108, as shown in Figure 8. For 1.9 and 3.1

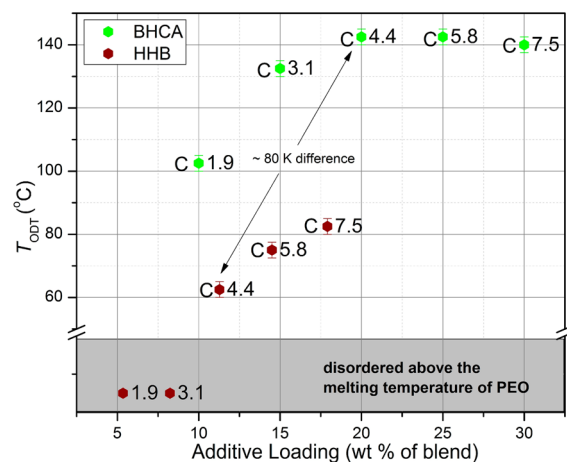


**Figure 8.** Order-to-disorder transition temperature ( $T_{ODT}$ ) dependence on additive loading for blends containing Pluronic F108 (F108) and two different additives from Figure 1, BHCA and HHB. Character “C” next to the data point represents cylindrical morphology of the blend at 60 °C. The digit next to each data point represents milliequivalents of functional group (carboxyl in case of BHCA and hydroxyl in case of HHB) incorporate per gram of F108 in the blend.

mequiv of functional groups per gram of F108, blends with HHB are still in a disordered state above melting point of PEO. At 4.4 mequiv functional group loading per gram of F108,  $T_{ODT}$  for HHB blends is lower by 80 K than of BHCA blends, indicating much higher segregation strength in BHCA blends. Simulated Connolly solvent excluded volumes of these molecules are 88 Å<sup>3</sup> and 164 Å<sup>3</sup> for HHB and BHCA respectively.<sup>48</sup> Since the size of the core benzene ring is unchanged, differences between filler volumes originate from the larger size of the carboxyl group compared to the hydroxyl group. For the same number of enthalpic interactions, the volumetric penalty is significantly larger in case of BHCA blends as compared to HHB. Still, the capacity of BHCA to induce phase segregation in F108 is significantly higher than of HHB. This is due to stronger hydrogen bonding of ether-oxygen of PEO segments with more electron deficient proton of the carboxyl group, compared to hydrogen bonding with the less electron deficient proton of the hydroxyl group. As mentioned earlier, BHCA blends are no longer homogeneous for loadings above 30 wt %, and comparison with HHB is no longer valid after this point.

## CONCLUSION

Small molecule additives bearing multiple hydrogen bonding sites can induce microphase separation in otherwise disordered F108. The additive molecules consist of carboxyl or hydroxyl

functional groups attached to a benzene ring. The hydrogen bonding between these functional groups and the PEO chains of F108 increase the effective  $\chi$  parameter between PEO and PPO chains thereby leading to microphase separation. The rich phase behavior of these F108/small-molecule-additive complexes depends upon loading of additive, temperature, and number of functional groups on the additive molecule.

Additives with six carboxyl groups surrounding an aromatic core (BHCA) show the strongest tendency to strengthen microphase separation.  $T_{ODT}$  increases steadily with BHCA loading in the blend and levels off at about 20 wt % loading. Unlike the common behavior of increasing solubility of small molecules with temperature, here we find that for high loadings the additives tend to self-interact and crystallize out upon increasing temperature. This is attributed to a weakening of hydrogen bonds between additive molecules and PEO chains. These crystallites formed at high temperature cause an increase in modulus due to reinforcement effects.  $T_{ODT}$  notably drops upon decreasing the number of hydrogen bonding functionalities on the additive core while keeping the total number of hydrogen bond donating functional groups approximately constant. Upon reducing the number of carboxyl groups from 6 to 5 and from 6 to 3, the  $T_{ODT}$  decreases by  $\sim 20$  and  $\sim 80$  °C, respectively. Using these small molecules as models, we find that carboxyl functionalized additives raise the  $T_{ODT}$  more effectively than hydroxyl functionalized additives.

## ■ ASSOCIATED CONTENT

### ● Supporting Information

SAXS and isothermal frequency sweep for F108, isothermal frequency sweep for 65/35 PEO/BHCA blend, optical micrograph for 75/25 F108/BHCA blend, and SAXS profile for 60/40 F108/BHCA blend. This material is available free of charge via the Internet at <http://pubs.acs.org>.

## ■ AUTHOR INFORMATION

### Corresponding Author

\*E-mail: [watkins@polysci.umass.edu](mailto:watkins@polysci.umass.edu) (J.J.W.).

### Notes

The authors declare no competing financial interest.

## ■ ACKNOWLEDGMENTS

Funding for this research was provided by National Science Foundation through the Center for Hierarchical Manufacturing (CMMI-1025020) at UMass Amherst. R.K. would like to acknowledge assistance with sample preparation from Dr. Vikram Daga and assistance with rheometer from Dr. Ahmed Khalil at the initial stage of this research.

## ■ REFERENCES

- (1) Leibler, L. Theory of Microphase Separation in Block Copolymers. *Macromolecules* **1980**, *13*, 1602–1617.
- (2) Bates, F. S.; Fredrickson, G. H. Block Copolymer Thermodynamics: Theory and Experiment. *Annu. Rev. Phys. Chem.* **1990**, *41*, 525–557.
- (3) Bates, F. S.; Fredrickson, G. H. Block Copolymers—Designer Soft Materials. *Phys. Today* **1999**, *52* (2), 32–38.
- (4) Hong, S. W.; Huh, J.; Gu, X.; Lee, D. H.; Jo, W. H.; Park, S.; Xu, T.; Russell, T. P. Unidirectionally aligned line patterns driven by entropic effects on faceted surfaces. *Proc. Natl. Acad. Sci. U.S.A.* **2012**, *109*, 1402–1406.
- (5) Ruiz, R.; Kang, H. M.; Detcheverry, F. A.; Dobisz, E.; Kercher, D. S.; Albrecht, T. R.; de Pablo, J. J.; Nealey, P. F. Density Multiplication

and Improved Lithography by Directed Block Copolymer Assembly. *Science* **2008**, *321*, 936–939.

- (6) Bitá, I.; Yang, J. K. W.; Jung, Y. S.; Ross, C. A.; Thomas, E. L.; Berggren, K. K. Graphoepitaxy of Self-Assembled Block Copolymers on Two-Dimensional Periodic Patterned Templates. *Science* **2008**, *321*, 939–943.

- (7) Cheng, J. Y.; Ross, C. A.; Chan, V. Z.; Thomas, E. L.; Lammertink, R. G. H.; Vancso, G. J. Formation of a Cobalt Magnetic Dot Array via Block Copolymer Lithography. *Adv. Mater.* **2001**, *13*, 1174–1178.

- (8) La, Y. H.; In, I.; Park, S. M.; Meagley, R. P.; Leolukman, M.; Gopalan, P.; Nealey, P. F. Pixelated chemically amplified resists: Investigation of material structure on the spatial distribution of photoacids and line edge roughness. *J. Vac. Sci. Technol. B* **2007**, *25*, 2508–2513.

- (9) Park, M.; Harrison, C.; Chaikin, P. M.; Register, R. A.; Adamson, D. H. Block Copolymer Lithography: Periodic Arrays of  $\sim 10^{11}$  Holes in 1 Square Centimeter. *Science* **1997**, *276*, 1401–1404.

- (10) Jeong, U.; Kim, H.-C.; Rodriguez, R. L.; Tsai, I. Y.; Stafford, C. M.; Kim, J. K.; Hawker, C. J.; Russell, T. P. Asymmetric Block Copolymers with Homopolymers: Routes to Multiple Length Scale Nanostructures. *Adv. Mater.* **2002**, *14*, 274–276.

- (11) Chan, V. Z.-H.; Hoffman, J.; Lee, V. Y.; Iatrou, H.; Avgeropoulos, A.; Hadjichristidis, N.; Miller, R. D.; Thomas, E. L. Ordered Bicontinuous Nanoporous and Nanorelief Ceramic Films from Self Assembling Polymer Precursors. *Science* **1999**, *286*, 1716–1719.

- (12) Lopes, W. A.; Jaeger, H. M. Hierarchical self-assembly of metal nanostructures on diblock copolymer scaffolds. *Nature* **2001**, *414*, 735–738.

- (13) Kim, H.-C.; Jia, X.; Stafford, C. M.; Kim, D. H.; McCarthy, T. J.; Tuominen, M.; Hawker, C. J.; Russell, T. P. A Route to Nanoscopic SiO<sub>2</sub> Posts via Block Copolymer Templates. *Adv. Mater.* **2001**, *13*, 795–797.

- (14) Pai, R. A.; Humayun, R.; Schulberg, M. T.; Sengupta, A.; Sun, J.-N.; Watkins, J. J. Mesoporous Silicates Prepared Using Preorganized Templates in Supercritical Fluids. *Science* **2004**, *303*, 507–510.

- (15) Tirumala, V. R.; Pai, R. A.; Agarwal, S.; Testa, J. J.; Bhatnagar, G.; Romang, A. H.; Chandler, C.; Gorman, B. P.; Jones, R. L.; Lin, E. K.; Watkins, J. J. Mesoporous Silica Films with Long-Range Order Prepared from Strongly Segregated Block Copolymer/Homopolymer Blend Templates. *Chem. Mater.* **2007**, *19*, 5868–5874.

- (16) Nagarajan, S.; Li, M. Q.; Pai, R. A.; Bosworth, J. K.; Busch, P.; Smilgies, D. M.; Ober, C. K.; Russell, T. P.; Watkins, J. J. An Efficient Route to Mesoporous Silica Films with Perpendicular Nanochannels. *Adv. Mater.* **2008**, *20*, 246–251.

- (17) Bladon, P.; Griffin, A. C. Self-Assembly in Living Nematics. *Macromolecules* **1993**, *26*, 6604–6610.

- (18) Alexander, C.; Jariwala, C. P.; Lee, C. M.; Griffin, A. C. Self-Assembly of Main Chain Liquid Crystalline Polymers Via Heteromeric Hydrogen Bonding. *Macromol. Symp.* **1994**, *77*, 283–293.

- (19) Lehn, J.-M. Supramolecular Chemistry—Molecular Information and the Design of Supramolecular Materials. *Macromol. Symp.* **1993**, *69*, 1–17.

- (20) Fouquey, C.; Lehn, J.-M.; Levelut, A.-M. Molecular recognition directed self-assembly of supramolecular liquid crystalline polymers from complementary chiral components. *Adv. Mater.* **1990**, *2*, 254–257.

- (21) Kihara, H.; Kato, T.; Uryu, T.; Fréchet, J. M. J. Supramolecular Liquid-Crystalline Networks Built by Self-Assembly of Multifunctional Hydrogen-Bonding Molecules. *Chem. Mater.* **1996**, *8*, 961–968.

- (22) Kihara, H.; Kato, T.; Uryu, T.; Fréchet, J. M. J. Induction of a cholesteric phase via self-assembly in supramolecular networks built of non-mesomorphic molecular components. *Liq. Cryst.* **1998**, *24*, 413–418.

- (23) Kato, T.; Fréchet, J. M. J. Stabilization of a Liquid-Crystalline Phase through Noncovalent Interaction with a Polymer Side Chain. *Macromolecules* **1989**, *22*, 3818–3819.

- (24) Araki, K.; Kato, T.; Kumar, U.; Fréchet, J. M. J. Dielectric properties of a hydrogen-bonded liquid-crystalline side-chain polymer. *Macromol. Rapid Commun.* **1995**, *16*, 733–739.
- (25) Bazuin, C. G.; Brandys, F. A. Novel Liquid-Crystalline Polymeric Materials via Noncovalent "Grafting". *Chem. Mater.* **1992**, *4*, 970–972.
- (26) Brandys, F. A.; Bazuin, C. G. Mixtures of an Acid-Functionalized Mesogen with Poly(4-vinylpyridine). *Chem. Mater.* **1996**, *8*, 83–92.
- (27) Stewart, D.; Imrie, C. T. Supramolecular Side-chain Liquid-crystal Polymers. *J. Mater. Chem.* **1995**, *5*, 223–228.
- (28) Malik, S.; Dhal, P. K.; Mashelkar, R. A. Hydrogen-Bonding-Mediated Generation of Side chain Liquid Crystalline Polymers from Complementary Nonmesogenic Precursors. *Macromolecules* **1995**, *28*, 2159–2164.
- (29) Ruokolainen, J.; Makinen, R.; Torkkeli, M.; Makela, T.; Serimaa, R.; ten Brinke, G.; Ikkala, O. Switching Supramolecular Polymeric Materials with Multiple Length Scales. *Science* **1998**, *280*, 557–560.
- (30) Ruokolainen, J.; Saariaho, M.; Ikkala, O.; ten Brinke, G.; Thomas, E. L.; Torkkeli, M.; Serimaa, R. Supramolecular Routes to Hierarchical Structures: Comb-Coil Diblock Copolymers Organized with Two Length Scales. *Macromolecules* **1999**, *32*, 1152–1158.
- (31) Chao, C. Y.; Li, X.; Ober, C. K. Directing Self-assembly in Macromolecular Systems: Hydrogen Bonding in Ordered Polymers. *Pure Appl. Chem.* **2004**, *76*, 1337–1343.
- (32) Ruokolainen, J.; ten Brinke, G.; Ikkala, O. Supramolecular Polymeric Materials With Hierarchical Structure-Within-Structure Morphologies. *Adv. Mater.* **1999**, *11*, 777–780.
- (33) Bondzic, S.; Wit, J. d.; Polushkin, E.; Schouten, A. J.; ten Brinke, G.; Ruokolainen, J.; Ikkala, O.; Dolbnya, I.; Bras, W. Self-Assembly of Supramolecules Consisting of Octyl Gallate Hydrogen Bonded to Polyisoprene-block-poly(vinylpyridine) Diblock Copolymers. *Macromolecules* **2004**, *37*, 9517–9524.
- (34) Tung, S. H.; Kalarickal, N. C.; Mays, J. W.; Xu, T. Hierarchical Assemblies of Block-Copolymer-Based Supramolecules in Thin Films. *Macromolecules* **2008**, *41*, 6453–6462.
- (35) van Zoelen, W.; Asumaa, T.; Ruokolainen, J.; Ikkala, O.; ten Brinke, G. Phase Behavior of Solvent Vapor Annealed Thin Films of PS-*b*-P4VP(PDP) Supramolecules. *Macromolecules* **2008**, *41*, 3199–3208.
- (36) Osuji, C.; Chao, C.-Y.; Bitá, I.; Ober, C. K.; Thomas, E. L. Temperature-Dependent Photonic Bandgap in a Self-Assembled Hydrogen-Bonded Liquid-Crystalline Diblock Copolymer. *Adv. Funct. Mater.* **2002**, *12*, 753–758.
- (37) Daga, V. K.; Watkins, J. J. Hydrogen-Bond-Mediated Phase Behavior of Complexes of Small Molecule Additives with Poly-(ethylene oxide-*b*-propylene oxide-*b*-ethylene oxide) triblock Copolymer Surfactants. *Macromolecules* **2010**, *43*, 9990–9997.
- (38) Tirumala, V. R.; Romang, A.; Agarwal, S.; Lin, E. K.; Watkins, J. J. Well Ordered Polymer Melts from Blends of Disordered Triblock Copolymer Surfactants and Functional Homopolymers. *Adv. Mater.* **2008**, *20*, 1603–1608.
- (39) Lin, Y.; Daga, V. K.; Anderson, E. R.; Gido, S. P.; Watkins, J. J. Nanoparticle-Driven Assembly of Block Copolymers: A Simple Route to Ordered Hybrid Materials. *J. Am. Chem. Soc.* **2011**, *133*, 6513–6516.
- (40) Yao, L.; Lin, Y.; Watkins, J. J. Ultrahigh Loading of Nanoparticles into Ordered Block Copolymer Composites. *Macromolecules* **2014**, *47*, 1844–1849.
- (41) Bates, F. S. Block Copolymers near the Microphase Separation Transition. 2. Linear Dynamic Mechanical Properties. *Macromolecules* **1984**, *17*, 2607–2613.
- (42) Balsara, N. P.; Perahia, D.; Safinya, C. R.; Tirrell, M.; Lodge, T. P. Birefringence Detection of the Order-to-Disorder Transition in Block Copolymer Liquids. *Macromolecules* **1992**, *25*, 3896–3901.
- (43) Winter, H. H.; Scott, D. B.; Gronski, W.; Okamoto, S.; Hashimoto, T. Ordering by Flow near the Disorder-Order Transition of a Triblock Copolymer Styrene-Isoprene-Styrene. *Macromolecules* **1993**, *26*, 7236–7244.
- (44) Fredrickson, G. H.; Bates, F. S. Dynamics of Block Copolymers—Theory and Experiment. *Annu. Rev. Mater. Sci.* **1996**, *26*, 501–550.
- (45) Yamaguchi, D.; Hashimoto, T.; Han, C. D.; Baek, D. M.; Kim, J. K.; Shi, A.-C. Order-Disorder Transition, Microdomain Structure, and Phase Behavior in Binary Mixtures of Low Molecular Weight Polystyrene-*block*-polyisoprene Copolymers. *Macromolecules* **1997**, *30*, 5832–5842.
- (46) Hahn, H.; Chakraborty, A. K.; Das, J.; Pople, J. A.; Balsara, N. P. Order-Disorder Transitions in Cross-Linked Block Copolymer Solids. *Macromolecules* **2005**, *38*, 1277–1285.
- (47) Winter, H. H. Three Views of Viscoelasticity for Cox-Merz Materials. *Rheol. Acta* **2009**, *48*, 241–243.
- (48) CS ChemDraw Ultra 11.0 Software.
- (49) Gilli, P.; Pretto, L.; Bertolasi, V.; Gilli, G. Predicting Hydrogen-Bond Strengths from Acid-Base Molecular Properties. The pK<sub>a</sub> Slide Rule: Toward the Solution of a Long-Lasting Problem. *Acc. Chem. Res.* **2009**, *42*, 33–44.
- (50) Vairam, S.; Govindarajan, S. New Hydrazinium Salts of Benzene Tricarboxylic and Tetracarboxylic Acids—Preparation and Their Thermal Studies. *Thermochim. Acta* **2004**, *414*, 263–270.
- (51) Brown, H. C.; Baude, E. A.; Nachod, F. C.; *Determination of Organic Structures by Physical Methods*; Academic Press: New York, 1955.